Two- and Three-Body Effects in Single Ionization of Li by 95 MeV/u Ar^{18+} Ions: Analogies with Photoionization

N. Stolterfoht, J.-Y. Chesnel, and M. Grether
Hahn-Meitner-Institut Berlin GmbH, Bereich Festkörperphysik, D-14109 Berlin, Germany

B. Skogvall
Technische Universität Berlin, Hardenbergstrasse 36, D-10623 Berlin, Germany

F. Frémont, D. Lecler, D. Hennecart, and X. Husson
Laboratoire de Spectroscopie Atomique, Institut des Sciences de la Matiere et du Rayonnement, F-14050 Caen, France

J. P. Grandin
Centre Interdisciplinaire de Recherche avec les Ions Lourds, CEA-CNRS, F-14070 Caen Cedex 5, France

B. Sulik and L. Gulyás
Institute of Nuclear Research (ATOMKI), H-4001 Debrecen, Hungary

J. A. Tanis
Western Michigan University, Kalamazoo, Michigan 49008
(Received 13 January 1998)

Cross sections for single electron emission have been measured in collisions of 95 MeV/u Ar^{18+} with atomic Li for electron energies 5–1000 eV and angles 25°–155°. The high projectile velocity made possible the separation of two- and three-body processes in the angular distributions of the ejected electrons. Low-energy emission of the $2s$ electrons is found to be significantly influenced by two-body effects and, furthermore, the node in the Li $2s$ wave function manifests itself in the angular spectra. Emission of $1s$ electrons is attributed mainly to three-body effects. The two- and three-body processes are associated with Compton scattering and photoabsorption, respectively. [S0031-9007(98)06108-0]

PACS numbers: 34.50.Fa, 32.80.Fb

Electron emission from a target atom by impact of a heavy projectile is a fundamental manifestation of the ionization process [1,2]. Electrons emitted with low energies are particularly important because these electrons have, by far, the largest probability for ejection. These low-energy electrons, referred to as soft-collision electrons, are produced mainly in large impact-parameter collisions. When the velocity of the projectile is much larger than the velocity of the active bound electron, the momentum transfer in a soft collision is small and the interaction of the ion with the target resembles that of a photon. The similarities in ionization by photons and charged particles have been recognized since the very beginning of atomic collision physics [3,4] and have subsequently been examined in detail [1,5,6]. Recently, considerable interest has been devoted to this subject [7–10].

The emission of slow electrons from an atom by the interaction with a photon comes about by means of the photoeffect where the incident photon is annihilated. In order to conserve energy and momentum the annihilation of a photon cannot take place without the interaction of the electron with the residual ion. Therefore, the photoeffect necessarily corresponds to a three-body process involving the incident photon, the active electron, and the residual target ion. It is well known that this interaction is mediated by a dipole transition involving the transfer of one unit angular momentum ($l = 1$). Because of the uncertainty principle the small angular momentum transfer corresponds to a broad angular distribution, symmetric around 90°, of the ejected electron [11].

With the similarities between fast ion and photon interactions in mind, the emission of soft-collision electrons is usually attributed to three-body effects between the projectile, the electron, and the target ion. On the other hand, for larger momentum transfer, two-body interactions involving binary-encounter processes become important. The two-body approximation and, thus, the neglect of the interaction with the residual ion is adopted in the framework of the impulse approximation [12,13].

As pointed out by Bethe [3], the two-body process in electron emission by ions is analogous to the Compton scattering of photons. Accordingly, the energy spectra of the binary-encounter electrons exhibit a pronounced peak whose shape is determined by the Compton profile of the corresponding bound orbital [14,15]. The binary encounter mechanism may also produce a distinct peak near 90° in the angular distribution of the ejected electrons involving high-order multipoles ($l \gg 1$) [11]. An important

criterion to observe such a sharp binary-encounter peak is the validity of the impulse approximation which, in turn, requires projectiles with a large velocity.

Thus, for fast projectiles two-body effects in ionization should produce a sharp peak, while three-body effects give rise to a broad angular distribution of the ejected electrons. These characteristic differences in the angular distributions of the binary- and soft-collision electrons provide an experimental method to separate the two- and three-body effects. For low-energy electron emission the important quantity which affects two- and three-body aspects in the ionization process is the binding energy of the active electron [2]. When the initial binding is large, the interaction of the outgoing electron with the residual ion is expected to be large also during the collision.

In previous studies, He for which the binding energy of the outermost electron is the highest of any atom has often been used as a target. Hence, for electron emission from He, three-body effects are expected to be most significant. For example, the emission of soft-collision electrons in relativistic collisions of U^{92+} with He was uniquely attributed to three-body, dipole-type transitions [10]. However, this supposition may not be valid for the more general case of a target atom with less tightly bound electrons. Furthermore, structures in the wave function, more complex than those of the $1s$ electron, may become important.

In this regard, we consider electron emission from Li which has two orbitals, $1s$ and $2s$, with largely different binding energies. The densities and wave functions [16] of these orbitals are shown in Fig. 1. The $1s$ electron has a binding energy of about 59 eV and is localized close (<1 a.u.) to the nucleus. The $2s$ electron has a much smaller binding energy of about 5.5 eV. Because of the node in the wave function, the $2s$ orbital has two parts, an inner part close to the nucleus (<1 a.u.) and an outer part extending quite far from the nucleus (up to about 7 a.u.). Thus, atomic Li provides a unique system in which to test effects of the binding energy and the wave function structure.

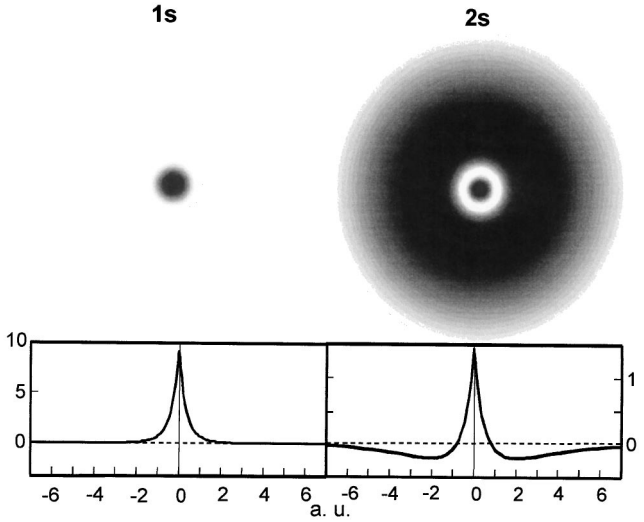

FIG. 1. Electron densities (upper part) and wave functions (lower part) for the atomic orbitals $1s$ and $2s$ of Li evaluated using the Cowan code [16].

In the present work, we study the collision system 95 MeV/u Ar^{18+} + Li where the projectile velocity is nearly equal to half the velocity of light ($v/c = 0.42$). It is shown that two- and three-body effects can, in fact, be separately identified in the angular distributions of the ejected electrons. Specifically, we found that three-body effects dominate the ionization of the $1s$ electron while two-body effects are primarily manifested in the ionization of the $2s$ electrons.

The measurements were carried out at the Grand Accélérateur National d'Ions Lourds accelerator facility in Caen, France. A beam of 95 MeV/u Ar^{18+} ions of intensity $1-2$ μA, collimated to a size of about 2 mm $\times$ 2 mm, was incident on a Li vapor jet target of $\sim$4 mm diameter obtained by heating metallic Li in a temperature controlled oven. Continuum electrons emitted from the Li were measured with a parallel-plate electron spectrometer for energies ranging from about 5–1000 eV, and for angles ranging from 25°–155°. The scattering chamber and the electron spectrometer were similar to those described previously [17].

When working with the lithium vapor target various instrumental difficulties had to be solved. The metallic lithium was heated slowly, thereby driving contaminations from the surface, until a stable lithium vapor beam was obtained. For the reliable detection of low-energy electrons, the possibility of perturbing effects due to the electric and magnetic fields associated with the relatively large current used to heat the metallic lithium, as well as effects due to lithium buildup on the spectrometer surfaces, must be considered. In the former case, measurements were taken with the heating current on and off, and in the latter case, an efficient baffle system was used to protect the sensitive parts of the spectrometer. With the procedures used, electron yields could be measured reliably for emission energies as low as 5 eV.

From the measured data we determined cross sections differential in energy ϵ and angle θ of the ejected electrons. To obtain absolute cross sections we normalized the angle-integrated data to the corresponding Rutherford cross sections [1,2]. Angular distributions for selected electron energies from 10 to 300 eV are shown in Fig. 2. It is noted that the measured data represent the sum of the electron emission from both the $1s$ and $2s$ orbitals. The individual contributions from these shells can be separated by model calculations as will be shown in the theoretical analysis below.

The double-differential cross section for electron emission can be expressed as a coherent sum of multipoles over the final state [18]:

$$\frac{d\sigma}{d\epsilon\, d\Omega} = \left| \sum_{lm} a_{lm} Y_{lm}(\theta) \right|^2, \qquad (1)$$

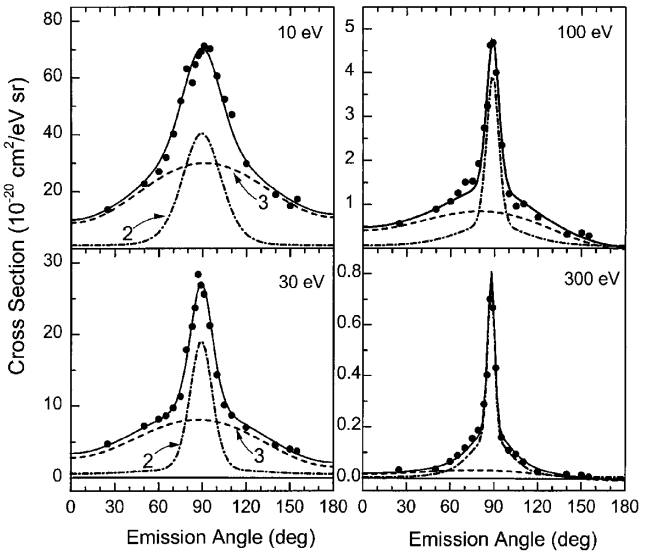

FIG. 2. Angular distributions of electrons emitted at energies of 10, 30, 100, and 300 eV. The dot-dashed curve labeled 2 refers to calculations using the two-body theory given by Eq. (2). The dashed curve labeled 3 is a fit to the underlying three-body part using the extended dipole term $A + B\sin^2\theta + C\cos\theta$ (see text). The solid curve is the sum of the two dashed curves.

where Y_{lm} are spherical harmonics and a_{lm} are amplitudes for electron emission with angular momentum l and magnetic quantum number m.

To treat the three-body part of the interaction we used the dipole term for $l = 1$ from Eq. (1). Hence, the angular distribution reduces to $A + B\sin^2\theta$, where the constants A and B are given by the amplitudes a_{10} and $a_{1\pm1}$. Since the smooth component of the angular distribution (three-body part) exhibits small asymmetries, we also kept the monopole term $l = 0$ which gives the cross term $C\cos\theta$ due to an interference effect with the dipole term. As shown below the monopole term is small due to the high projectile energy used in this work. Therefore, for brevity, the sum of monopole and dipole terms will be referred to as an extended dipole term.

Applying the impulse and peaking approximations [2,14] within the framework of the Born approximation, the two-body part of the interaction can be represented by a simple expression including the Compton profile $J(p_z)$

$$\frac{d\sigma}{d\epsilon\, d\Omega} = \frac{4Z_p^2}{v^2 k_c^3} J(p_z), \qquad (2)$$

where Z_p is the projectile charge, $p_z = k\cos\theta - \Delta E/v$ is the initial momentum component along the beam direction, and $k = \sqrt{2\epsilon}$ is the ejected electron momentum. The momentum $k_c = \sqrt{2\Delta E}$ is derived from the energy loss $\Delta E = \epsilon + E_b$, where E_b is the binding energy of the active electron. Note that $k_c \approx k$ for $\epsilon \gg E_b$.

Theoretical results are compared with the experimental data in Fig. 2. The two-body part (dot-dashed curve) is evaluated using Eq. (2). After subtraction of the two-body part, the extended dipole term (dashed curve) is fit to the experimental data taken primarily at forward ($\leq 60°$) and backward angles ($\geq 120°$). The sum of these two theoretical components (solid curve) compares very well the experimental data.

The results presented in Fig. 2 show that the two- and three-body parts change considerably in magnitude as the electron energy varies. For 10 eV electrons the two- and three-body contributions to ionization are nearly equal while for 300 eV electrons the two-body theory accounts for nearly all of the electron emission. This former finding is remarkable. Since the pioneering work of Bethe [3] it has become common practice to attribute the emission of low-energy electrons by fast projectiles to three-body dipole transitions [5,6,9,10]. On the contrary, the present results illustrate convincingly the point made earlier that two-body interactions become important for low-energy emission of less tightly bound electrons.

The two-body part of the interaction manifests itself as a distinct binary-encounter peak centered near 90° which represents the Compton profile of the target electrons. The increasing sharpness of the Compton profile with increasing electron energies may readily be understood from the derivative of the above expression for the initial momentum p_z, yielding for the angular width $\Delta\theta = \Delta p_z/k$ (setting $\sin\theta \approx 1$ at angles near 90°). Hence, for a given Δp_z it follows that the angular width $\Delta\theta$ decreases with increasing electron momentum k.

An important consequence of Eq. (2) is that nearly all of the two-body ionization can be attributed to the $2s$ orbital. (The $1s$ contribution becomes noticeable only at higher electron energies, e.g., at 300 eV.) Furthermore, the inner part of the $2s$ wave function, since it is closer to the nucleus, has a broader Compton profile than the outer part of the $2s$ wave function which is spatially distributed much farther from the nucleus. Thus, the effect of the node in the $2s$ orbital (Fig. 1) is to give rise to a "kink" in the Compton profile, confirmed by the experiment, which can be clearly seen in the 100 and 300 eV spectra.

Another remarkable result of the spectral analysis is that at high electron emission energies the three-body part of the ionization process can be separated from the dominating two-body part. To study further the properties of the three-body interaction, in particular, the $1s$ and $2s$ contributions, theoretical results for individual multipoles have been evaluated within the framework of the Born approximation using a modified version of the program by Gulyás *et al.* [19]. The double-differential cross sections were integrated over the electron emission angle. This integration cancels the interferences between multipoles (e.g., monopole and dipole) so that the multipole terms become fully separable.

In Fig. 3 the fitted experimental data are compared with theoretical results for dipole (plus monopole) transitions. (The theory confirms that the monopole term is much smaller than the dipole term.) The good agreement obtained between experiment and theory seen in Fig. 3 attests to the validity of attributing the fitted part of the

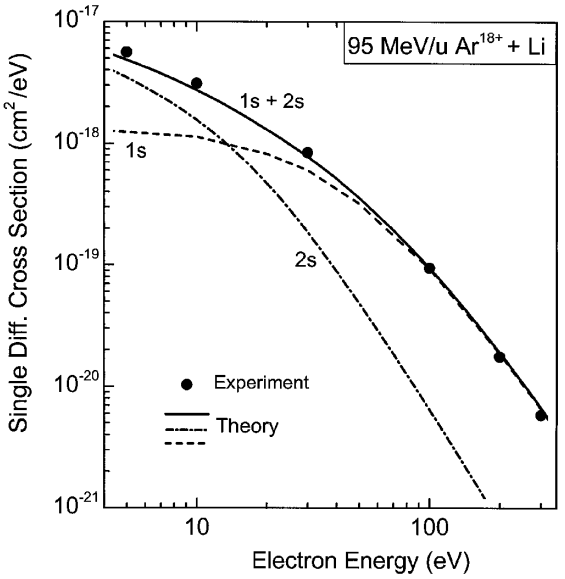

FIG. 3. Angle integrated cross sections for electron emission by dipole (plus monopole) transitions representing three-body processes. The data points originate from the fits to the experimental results shown in Fig. 2. The lines are calculations of transitions to final $l = 0$ and 1 states using the Born approximation [19]. The labels $1s$ and $2s$ refer to results for these orbitals.

experimental data to dipole transitions and, hence, to three-body effects. We also evaluated individual results for the $1s$ and $2s$ orbitals (Fig. 3). The relative $1s$ contribution to the three-body effects increases strongly as the ejected electron energy increases, and for electrons emitted with energies ≥ 50 eV, the $1s$ contribution accounts for nearly all of the three-body effects.

Lastly, returning to the analogy between fast ions and photons we note from the Einstein relation for the photoeffect that the present electron spectroscopy measurements allow for determining the energy of the annihilated (virtual) photon, i.e., this photon energy is equal to the electronic energy transfer $\Delta E = E_b + \epsilon$. The probability for photoabsorption decreases strongly with photon energy following the exponential law $\Delta E^{-3.5}$ [7,9]. This law can indeed be verified from the data in Fig. 3 showing that electron spectroscopy experiments with ion impact provide information about corresponding results for photoinization in a wide range of photon energies.

In conclusion, we have shown for very fast collisions that two- and three-body effects in the ionization process can be separated. For energies ≥ 100 eV electron emission near 90° is dominated almost totally by $2s$ ionization via two-body interactions. In contrast to He $1s$ ionization, for Li the two-body effects are found to be important for electron energies as low as 5 eV. Furthermore, at forward and backward angles electron emission due to three-body interactions is dominant, with the contribution from the $1s$ orbital becoming significantly more important as the energy of the emitted electron increases. Finally, we show that the analysis of three-body processes reveals characteristic information about photoionization.

This work was supported by the German-French Cooperation Programme PROCOPE and the German-Hungarian Intergovernmental Collaboration (Project No. B/129). J.-Y. C. was supported by the Alexander von Humboldt Foundation; B. S. was supported by the Hungarian National Science Fund (Contract No. OTKA-T-020-771) and by the Hungarian Academic Research Fund (AKP, Contract No. 96/665 2,2); J. A. T. was supported by the Division of Chemical Sciences, Office of Basic Energy Sciences, Office of Energy Research, U.S. Department of Energy.

[1] M. E. Rudd, Y.-K. Kim, D. H. Madison, and T. J. Gay, Rev. Mod. Phys. **64**, 441 (1992).
[2] N. Stolterfoht, R. D. DuBois, and R. D. Rivarola, *Electron Emission in Heavy Ion-Atom Collisions* (Springer-Verlag, Berlin, 1997).
[3] H. A. Bethe, Ann. Phys. (Leipzig) **5**, 325 (1930).
[4] E. J. Williams, Phys. Rev. **45**, 729 (1934).
[5] M. Inokuti, Rev. Mod. Phys. **43**, 297 (1971); M. Inokuti, Y. Itikawa, and J. E. Turner, Rev. Mod. Phys. **50**, 23 (1978).
[6] Y.-K. Kim, Phys. Rev. A **6**, 666 (1972); Y.-K. Kim and M. Inokuti, Phys. Rev. A **7**, 1257 (1973).
[7] J. Burgdörfer, L. R. Anderson, J. H. McGuire, and T. Ishihara, Phys. Rev. A **50**, 349 (1994).
[8] J. Wang, J. H. McGuire, J. Burgdörfer, and Y. Qiu, Phys. Rev. Lett. **77**, 1723 (1996).
[9] J. H. McGuire, *Introduction to Dynamic Correlation* (Cambridge University Press, Cambridge, England, 1997).
[10] R. Moshammer *et al.*, Phys. Rev. Lett. **79**, 3621 (1997).
[11] The angular momentum l and the emission angle θ are canonical quantities which are subject to the uncertainty principle $\Delta l \Delta\theta = 1$. Hence, low-order multipole transitions produce a broad angular distribution and vice versa.
[12] P. Eisenberger and P. M. Platzman, Phys. Rev. A **2**, 415 (1970).
[13] D. Brandt, Phys. Rev. A **27**, 1314 (1983).
[14] F. Bell, H. Böckl, M. Z. Wu, and H.-D. Betz, J. Phys. B **16**, 187 (1983).
[15] D. H. Lee *et al.*, Phys. Rev. A **41**, 4816 (1990).
[16] R. D. Cowan, *The Theory of Atomic Structure and Spectra* (University of California Press, Berkeley, 1981).
[17] N. Stolterfoht, Z. Phys. **248**, 81 (1971); N. Stolterfoht *et al.*, Europhys. Lett. **4**, 899 (1987).
[18] S. T. Manson, L. H. Toburen, D. H. Madison, and N. Stolterfoht, Phys. Rev. A **12**, 60 (1975).
[19] L. Gulyás, P. D. Fainstein, and A. Salin, J. Phys. B **28**, 245 (1995).